Biotechnol Lett (2017) 39:375–382
DOI 10.1007/s10529-016-2257-2

ORIGINAL RESEARCH PAPER

# Interactions of in vitro selected fluorogenic peptide aptamers with calmodulin

**Yasodha Manandhar · Wei Wang · Jin Inoue · Nobuhiro Hayashi · Takanori Uzawa · Yutaka Ito · Toshiro Aigaki · Yoshihiro Ito**

Received: 23 September 2016 / Accepted: 10 November 2016 / Published online: 17 November 2016


**Abstract**
*Objectives* We examined the importance of aptamer usage under the same condition as the selection process by employing the previously selected aptamers for calmodulin (CaM) which includes a non-natural fluorogenic amino acid, 7-nitro-2,1,3-benzoxadiazole.
*Results* We added five amino acids at the *N*-terminus which was employed for the selection and then we tested the affinity and selectivity for CaM binding. Surface plasmon resonance and fluorescence measurements showed that the additional amino acids for one of the aptamers drastically improved binding affinity to CaM, indicating the importance of aptamer use under the same conditions as the selection process. Such drastic improvement in affinity was not observed for the sequence which had been reported previously. Nuclear magnetic resonance data identified that the primary binding site is located in a *C*-terminal of CaM and the additional residues enhance interactions with CaM.
*Conclusions* We found that the addition of the common sequence, which was employed for ribosome display, makes the affinity of a selected peptide as strong as the previously reported peptide.

**Keywords** Calmodulin · Fluorescence · 7-nitro-2,1,3-benzoxadiazole · NMR · Signaling peptide aptamer · Surface plasmon resonance

Yasodha Manandhar and Wei Wang are contributed equally to this research work.

**Electronic supplementary material** The online version of this article (doi:10.1007/s10529-016-2257-2) contains supplementary material, which is available to authorized users.

Y. Manandhar · W. Wang · T. Uzawa · T. Aigaki · Y. Ito (✉)
Nano Medical Engineering Laboratory, RIKEN, 2-1 Hirosawa, Wako, Saitama 351-0198, Japan
e-mail: y-ito@riken.jp

Y. Manandhar · T. Aigaki · Y. Ito
Graduate School of Biological Science, Tokyo Metropolitan University, 1-1 Minami-Osawa, Tokyo 192-0397, Japan

J. Inoue · Y. Ito
Department of Chemistry, Tokyo Metropolitan University, 1-1 Minami-Osawa, Tokyo 192-0397, Japan

N. Hayashi
Department of Life Science and Technology, School of Life Science and Technology, Tokyo Institute of Technology, 2-12-1, Ookayama, Meguro-ku, Tokyo 152-8550, Japan

T. Uzawa · Y. Ito
Emergent Bioengineering Materials Research Team, RIKEN Center for Emergent Matter Science, 2-1 Hirosawa, Wako, Saitama 351-0198, Japan

## Introduction

Aptamers are functional oligonucleotides, proteins, or peptides isolated from very large random sequence libraries by in vitro selection based on the affinity to a desired specific target. Protein and peptide aptamers were first selected using phage display (Smith 1985) and subsequently using in vitro translation systems, including ribosome and mRNA displays (Hanes and Pluckthum 1997; Nemoto et al. 1997; Roberts and Szostak 1997). Canonical components (i.e., four nucleotides and 20 amino acids) and non-canonical moieties have been used for aptamers. In particular, the number of non-canonical moieties in the selection library has increased over the last decade (Uzawa et al. 2013; Lane and Seeling 2014; Dodevski et al. 2015; Maini et al. 2016).

For example, photo-isomerizable (Liu et al. 2012; Jafari et al. 2014; Bellotto et al. 2014), inhibitor (Li and Roberts 2003; Wang et al. 2014a, b), catechol (Wilke et al. 2014) and environment-sensitive fluorescence groups (Wang et al. 2014a, b; Manandhar et al. 2015; Wang et al. 2016) have been incorporated into aptamers. These functional groups add new artificial or additional functions to aptamers, which inherently have molecular recognition functions. The introduction of a photo-isomerizable group facilitated control of binding by photo-irradiation (Liu et al. 2012; Jafari et al. 2014; Bellotto et al. 2014), whereas the addition of an aptamer sequence to an inhibitor increased binding affinity by increasing the number of interaction sites (Li and Roberts 2003; Wang et al. 2014a, b). The introduction of an environment-sensitive fluorescence group enabled a fluorescence change upon binding a target molecule (Wang et al. 2014a, b; Manandhar et al. 2015; Wang et al. 2016). This fluorogenic aptamer technology realizes universal analysis of arbitrary targets without bound/free separation.

We reported previously the identification of fluorogenic peptides that bind to calmodulin (CaM) through selection using a combination of ribosome display and misaminoacylated, biorthogonal tRNA (Wang et al. 2014a, b). A hydrophobic indicator, 7-nitro-2,1,3-benzoxadiazole (NBD), that emits fluorescence in a hydrophobic environment was incorporated into the library. In this report, the behavior of a peptide among candidate peptides was investigated in detail. However, in this study, we found that the addition of a common sequence, which was employed for ribosome display (Supplementary Fig. 1), makes the affinity of another candidate peptide as strong as the previously reported peptide. Therefore, the binding behaviors of these peptides with the addition of this common sequence were characterized by fluorescence spectroscopy, surface plasmon resonance (SPR) and nuclear magnetic resonance (NMR). The additional sequence added to a peptide was found to reflect the interaction between target and a peptide-ribosome-mRNA complex during ribosome display.

## Materials and methods

### Solubility

The synthesized peptide solutions were super-saturated using a microdialysis device overnight in buffer (50 mM Tris/acetate, 150 mM KCl, 5 mM $CaCl_2$, pH 7.0). The saturated solutions were collected and centrifuged at 14,000 × *g* for 20 min to obtain the supernatant for absorbance measurement. The maximum absorbance was then measured for NBD and the concentration was calculated using the extinction coefficient of NBD at 485 nm ($\varepsilon_{max} = -19{,}500$ L/mol cm). The acidic, basic and hydrophobic sequence composition as percentages were calculated using the peptide property calculator LifeTein® online software program.

### Surface plasmon resonance (SPR) measurements

SPR measurements were performed on a Biacore T100 instrument with a CM5 sensor chip (GE Healthcare Bio-Science, Uppsala, Sweden). Bovine CaM purchased from Sigma Aldrich (St Louis, MO, USA) was immobilized on the CM5 sensor chip surface according to previous reports (Lin et al. 1974; Crouch and Klee 1980).

After immobilization of CaM onto the sensor surface, affinity analysis was carried out for the peptides. All the experiments were performed at 25 °C with a constant flow of 30 μL/min. For the affinity analysis, various concentrations of peptide solutions in buffer with 0.05% Tween 20 and 5 mM $CaCl_2$ were injected over the sensor chip containing the immobilized CaM. The sensor chip was regenerated by injection of 10 mM EGTA (pH 8.0) for 30 s, followed by buffer with 0.05% Tween 20 and 5 mM $CaCl_2$ for 5 min to stabilize the baseline. This

measurement was carried out only in the presence of $Ca^{2+}$. All of the binding curves were collected by subtraction of the curve for a reference flow cell and fitted to a steady state affinity model using the Biacore T100 Evaluation Software (version 2.0.3).

### Fluorescence measurements

Fluorescence measurements were performed excitation was at 488 nm and emission was measured from 500 to 600 nm: To determine the fluorescence intensity change, CaM from 0–16 μM was added to 2 μM MB4. Similarly, CaM from 0–30 μM was added to 5 μM of MC5 and MD9 peptides in buffer. Fluorescence intensity changes in the presence and absence of $Ca^{2+}$ were measured. For CaM binding to the peptides, the concentration of CaM was increased until a saturation level was obtained. The relative fluorescence intensity changes (RFIC) of peptides with CaM were calculated at the maximum emission wavelength of 535 nm. RFIC were calculated as $RFIC = (F_X - F_0)/F_0$, where $F_X$ and $F_0$ are the fluorescence intensity of a peptide with and without CaM, respectively. The calculated RFIC were plotted using Graph Pad Prism 5 (Graph Pad Software Inc., CA, USA) and the dissociation constant ($K_d$) values were estimated by non-linear regression analysis of the emission intensities at 535 nm.

### NMR measurements

For the NMR titration experiments of $^{15}N$-labelled human CaM with MB4, MC5 and MD9 peptide aptamers, a series of two-dimensional (2D) $^{1}H–^{15}N$ HSQC spectra were measured on $^{15}N$-labeled CaM (0.1 mM) at various protein:peptide ratios to monitor gradual changes in the chemical shifts or intensity of $^{1}H–^{15}N$ correlations. The $^{15}N$-labeled human CaM sample was purified using the protocols presented previously (Hayashi et al. 1998). $^{15}N$-Labelled CaM was dissolved in 50 mM Tris/HCl buffer (pH 7.5) containing 120 mM NaCl and 2.5 mM $CaCl_2$ and 10% $^{2}H_2O$. 2D $^{1}H–^{15}N$ HSQC spectra were acquired with eight transients and a total of 2048 ($t_2$, $^{1}H^{N}$) × 256 ($t_1$, $^{15}N$) complex points. Initially, a reference spectrum was recorded in the absence of peptides. Then the sample was mixed with 20 mM peptide to achieve a protein:peptide molar ratio of 1:0.5, prior to the next measurement. More peptide solution was added incrementally to measure 2D $^{1}H–^{15}N$ HSQC spectra at protein:peptide molar ratios of 1:1, 1:2 and 1:3. The concentration of the protein was not adjusted after each titration point because of the small volume of the peptide solution added. Details about NMR measurement system and backbone assignments are in the supporting information.

## Results and discussion

The selected peptides with five fixed residues, MAMQA, at the *N*-terminus, which derive from the restriction enzyme site during selection (Supplementary Fig. 1), were synthesized using the NBD labeled aminophenylalanine by solid phase peptide synthesis. We left the additional five amino acids in common, because the translational efficiency of a polypeptide largely depends on its *N*-terminal amino acids sequence. Ueno et al. (2012) proposed an elegant strategy to use a protease to generate the library whose *N*-terminus are randomized; however, the efficiency of protease activity would also depend on the library sequence.

### Solubility

The solubility of the peptides in an aqueous buffer and the calculated hydrophobic percentage of each synthesized peptide are presented in Table 1. The solubility was dependent on the sequence. Although the hydrophobic percentages were the same for peptides MB4 and MC5, the percentage of acidic and basic amino acids differed between the two peptides.

### SPR measurements

The binding properties of the peptide aptamers (MB4, MC5 and MD9) on immobilized CaM in the presence of $Ca^{2+}$ were performed by SPR (Supplementary Figs. 2, 3, 4). Table 2 presents the affinity analysis of the peptides using a steady state affinity model with dissociation constants given. MB4 and MC5 have similar affinity to CaM, whereas the affinity of MD9 was slightly lower.

### Fluorescence measurements

The fluorescence of the three peptides in the presence of calcium ions was measured (Supplementary Fig. 5). The increase in fluorescence intensity indicates that

**Table 1** Synthesized selected peptide sequences with solubility

| Synthetic peptides | Repetition[a] | Sequence[b] | Molecular weight | Calculated hydrophobic (%)[c] | Solubility (μM) |
|---|---|---|---|---|---|
| MB4 | 9 | MAMQASNIXYANKLRR | 2204.9 | 53 | 31.31 |
| MC5 | 4 | MAMQAYWDKIKDXIGG | 2164.8 | 53 | 126.6 |
| MD9 | 2 | MAMQADMASLVAXVMD | 2022.3 | 73 | 5.44 |

[a] Repetition, number of repetition of aptamer sequence out of 67 readable colonies

[b] X, NBD coupled phenylalanine

[c] The hydrophobic percentage was calculated using the 'Peptide property calculator-LifeTein®, online software excluding X, a non-natural amino acid

**Table 2** Peptides with $K_d$ (μM) values

| Synthetic peptides | $K_d$ (μM) | |
|---|---|---|
| | SPR | Fluorescence |
| MB4 | 0.6 ± 0.02 | 2.2 ± 0.25 |
| MC5 | 0.9 ± 0.05 | 5.7 ± 0.22 |
| MD9 | 7.5 ± 0.37 | 4.8 ± 0.28 |

the peptides bind in a hydrophobic pocket of CaM, that is exposed to $Ca^{2+}$. The fluorescent intensity of MB4 was extremely low in the absence of CaM and the wavelength of maximum fluorescence was 539 nm. The wavelength shifted to 532 nm as the concentration of CaM increased. Conversely, in the absence of CaM both MC5 and MD9 showed weak fluorescence. As observed for MB4, the wavelength of maximum fluorescence intensity of MC5 shifted from 541 to 531 nm and that of MD9 from 542 to 531 nm as the concentration of CaM increased. Although the initial fluorescence of each peptide differed, the shift in maximum fluorescence intensity was to the blue, and the width was between 7 and 10 nm. The blue shift demonstrated the hydrophobic interaction of the NBD moiety with CaM.

The relative fluorescence intensity changes (RFIC) of peptide with CaM were at 535 nm. In the presence of $Ca^{2+}$, the fluorescent signal of the MB4 peptide increased up to 16-fold with a concomitant increase in CaM to 10 μM (Fig. 1a). Although the fluorescence intensity of the corresponding peptide without the common sequence (B4 in the supporting information in Wang et al. 2014) was found to increase linearly, the presence of this common sequence drastically changed the behavior yielding a fluorescence increase for MB4, which is typically seen for specific binding. In the case of MC5 and MD9, the increase in fluorescence intensity was 3- and 3.5-fold, respectively (Fig. 1b, c). The $K_d$ between peptides and CaM were estimated from the results of Fig. 1, as shown in Table 2. The $K_d$ values of the three peptides were of the same order. Although the binding affinities of peptides are dependent on sequence, the micro-environmental change of NBD induced by the interaction with CaM was not dependent on the peptide sequence.

## NMR measurements

The binding mechanism of peptides MB4, MC5 and MD9 with CaM was characterized by a series of stepwise, multipoint NMR titration experiments using $^{15}N$-labeled human CaM (Fig. 2). Initially, a 2D $^{1}H$–$^{15}N$ HSQC was measured in the absence of peptides (zero concentration point) and then spectra at each peptide titration point were measured to identify the binding interface on CaM.

Titration of $^{15}N$-labeled CaM with MB4 peptide gave rise to chemical shift changes to a large number of resonances. We observed the disappearance and emergence of signals, indicating that the binding of CaM to MB4 was on the slow exchange timescale. The disappearance and emergence of resonances were observed at the first titration point (protein:peptide molar ratio of 1:0.5). A gradual increase in MB4 peptide concentration to saturate CaM protein (protein:peptide molar ratio of 1:3) gave rise to a large amount of precipitant and the change in chemical shifts of resonances was not saturated. Therefore, CaM and MB4 were mixed under diluted conditions (0.01 mM CaM with 0.03 mM MB4), and the sample was gradually concentrated using an ultrafiltration membrane. As a result, we observed saturation of

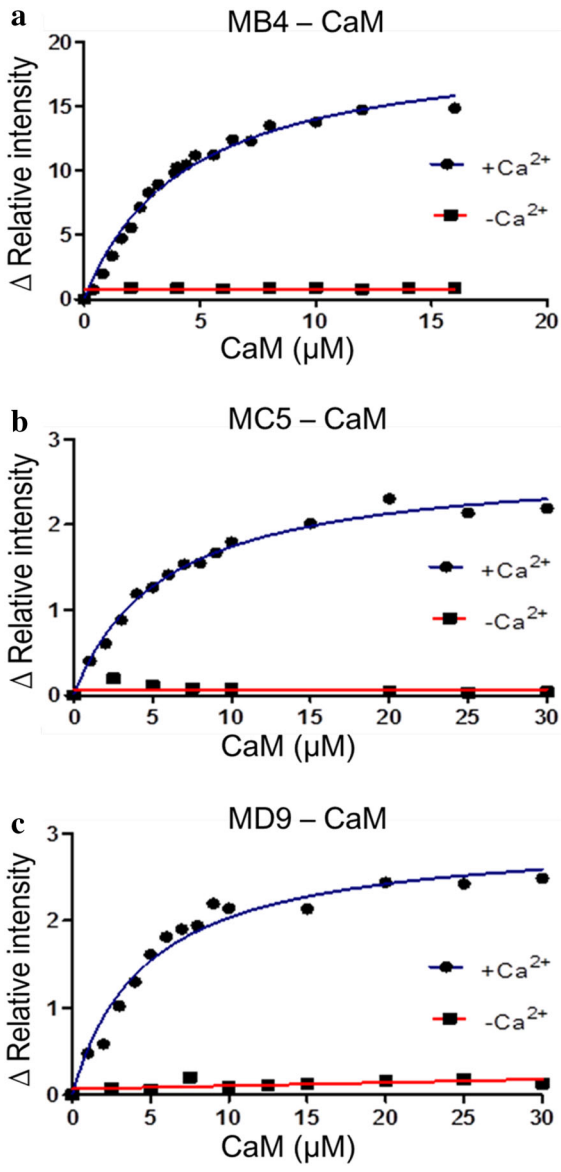


**Fig. 1** Data points fitted by the *blue line* represent the RFIC of $Ca^{2+}$ bound CaM at different concentrations and the *curve* shows the best fit to non-linear regression analysis of emission intensities at 535 nm. The *red line* containing data points shows the RFIC in the absence of $Ca^{2+}$ bound CaM

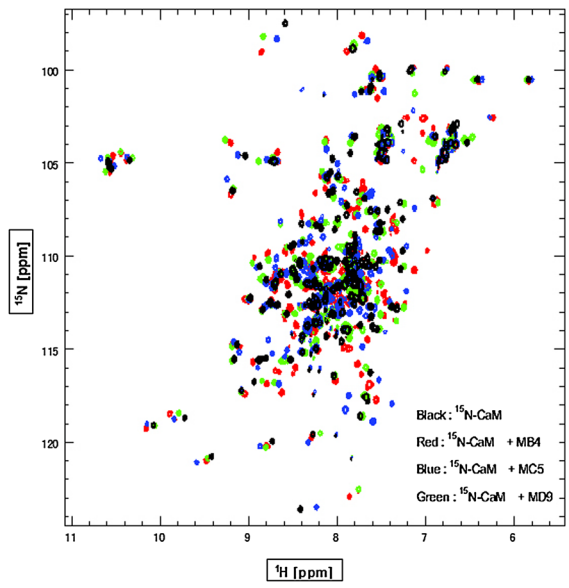


**Fig. 2** A 2D $^{1}H$–$^{15}N$ HSQC spectrum. Mapping of the affected residues by addition of the MC5 peptide on CaM in a ribbon diagram. Large chemical shift changes to resonances induced by the addition of MC5 are shown in *red*. Ala129, Asn138 and Glu140–Met145 are represented as stick models. $Ca^{2+}$ ions are shown as *magenta spheres*

chemical shift changes to resonances at a CaM:MB4 molar ratio of 1:3. NMR titration of $^{15}N$-labeled CaM with MC5 and MD9 peptides also gave the disappearance and emergence of signals, indicating that binding of CaM with these two peptides is also on the slow exchange timescale. The disappearance and emergence of resonances were observed at the first titration point (protein:peptide molar ratio of 1:0.5) and was almost saturated at a protein:peptide molar ratio of 1:3 (MC5) and 1:4 (MD9).

Due to the timescale of the interaction, it was difficult to follow chemical shift changes to resonances during the peptide titration experiments with assignment information for apo-CaM. Therefore, assignment of the backbone $^{1}HN$, $^{13}C^{\alpha}$, $^{13}C'$, $^{15}N$ and side-chain $^{13}C^{\beta}$ resonances of $^{13}C/^{15}N$-uniformly labeled CaM in the presence of the peptides was performed. By analyzing the spin–spin connectivity in the 3D triple-resonance NMR spectra, 67% of the backbone resonances (100/149 amino acids) were assigned in the presence of the MC5 peptide at the protein:peptide molar ratio of 1:3. In the case of MB4 and MD9 peptides, no assignment information of the backbone resonances of CaM was completed because the quality of the 3D NMR spectra was poor. This was due to the low solubility of the peptides, which caused field inhomogeneity and thus poor quality 3D spectra; although, peptide solubility was enhanced by the addition of the five residues at the *N*-terminus.

Large chemical shift changes induced by the addition of the MC5 peptide ($\Delta_{ave} > 80$ Hz) were found for residues Ser18, Phe20, Ile28, Val36, Met37,

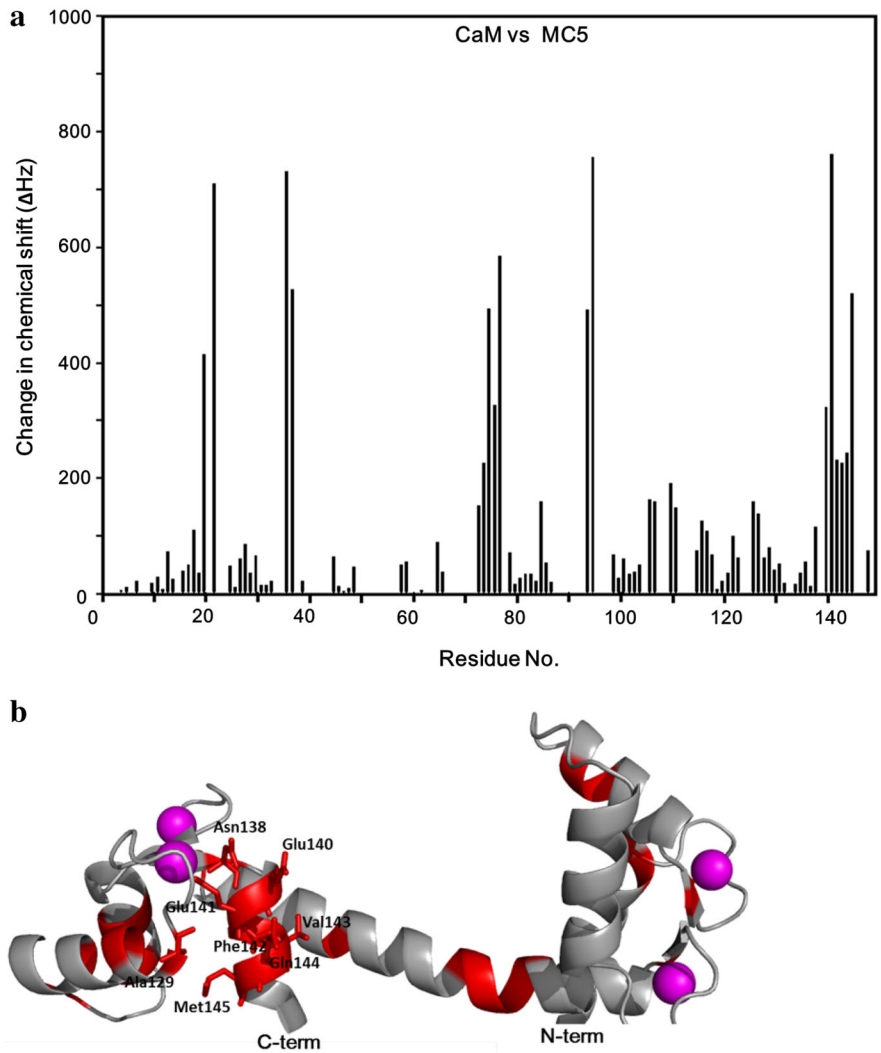


**Fig. 3** **a** Chemical shift changes to resonances representing CaM upon interaction with MC5. The chemical shift changes in both $^{1}H$ and $^{15}N$ were normalized by the equation $[(\Delta^{15}N_{Hz})^2 + (\Delta^{1}H_{Hz})^2]^{1/2}$. **b** The expected primary binding surface for the MC5 peptide

Phe65, Met73–Met77, Glu85, Asp94, Lys95, Leu106, Arg107, Met110, Thr111, Lys116, Leu117, Val122, Ile126, Arg127, Ala129, Asn138 and Glu140–Met145. These residues form a solvent exposed cluster. The residues affected by the addition of the MC5 peptide were mapped to the crystal structure of *Rattus rattus* CaM (PDB ID:3CLN). The mapping result shows that MC5 binding to CaM affects many regions of CaM; however, the changes to Ala129, Asn138 and between Glu140–Met145 were particularly large and clustered (Fig. 3a). This result indicates that residues Ala129, Asn138 and Glu140–Met145 furnish the primary binding surface for the MC5 peptide (Fig. 3b), and that the binding surface for MC5 is located in the *C*-terminal domain of CaM, which correlates with the results observed for the C5 peptide (Wang et al. 2014). For MB4 and MD9 binding, the NMR spectra obtained were compared with the NMR data for MC5, and this overlaying of spectral data showed that the changes in chemical shifts of resonances yielded a similar pattern, indicating that these three peptides bind a similar region located in the *C*-terminal domain of CaM.

CaM captures various kinds of molecules and targets are not restricted to proteins. Nevertheless, physical properties of the target ligands are conserved with most showing basic amphiphilicity (Hayashi and Titani 2010) and in the many cases CaM recognizes these ligand properties using a similar core region. Therefore, the similar resonance shift patterns of the

2D $^{1}H$–$^{15}N$ HSQC spectra obtained from the titration experiments of CaM with target peptides suggests that CaM uses a similar binding region as shown for other ligands, even though these three peptides do not display explicit basic amphiphilicity.

## Conclusion

Three major in vitro selected peptide sequences were synthesized by solid phase peptide synthesis. The interaction of the peptides with a target molecule was investigated by SPR, fluorescence and NMR spectroscopy. We found that the addition of the common sequence, which was employed for ribosome display, makes the affinity of another candidate peptide as strong as the previously reported peptide.

**Acknowledgements** This work was supported in part by the JSPS KAKENHI (Grant Numbers 22220009 and 15H01810).

**Supporting information** Supporting Methods—Peptide synthesis: NMR system and backbone assignments.

Supplementary Table 1—Peptides with $K_d$ (μM) values obtained from fluorescence with and without MAMQA sequence.

Supplementary Fig. 1—Synthesis of the nascent peptide with 'MAMQA' at the *N*-terminus.

Supplementary Fig. 2—SPR result of MB4.

Supplementary Fig. 3—SPR result of MC5.

Supplementary Fig. 4—SPR result of MD9.

Supplementary Fig. 5—The fluorescence emission spectra of the aptamers.

## References

Bellotto S, Chen S, Rebollo IR, Wegner HA, Heinis C (2014) Phage selection of photoswitchable peptide ligands. J Am Chem Soc 136:5880–5883

Crouch TH, Klee CB (1980) Positive cooperative binding of calcium to bovine brain calmodulin. Biochemistry 19:3692–3698

Dodevski I, Markou GC, Sakar CA (2015) Conceptual and methodological advances in cell-free directed evolution. Curr Opin Struct Biol 33:1–7

Hanes J, Pluckthum A (1997) In vitro selection and evolution of functional proteins by using ribosome display. Proc Natl Acad Sci USA 94:4937–4942

Hayashi N, Titani K (2010) N-myristoylated proteins, key components in intracellular signal transduction systems enabling rapid and flexible cell responses. Proc Jpn Acad Ser B 86:494–508

Hayashi N, Matsubara M, Takasaki A, Titani K, Taniguchi H (1998) An expression system of rat calmodulin using T7 phage promoter in *Escherichia coli*. Protein Expr Purif 12:25–28

Hayashi N, Izumi Y, Titani K, Matsushima N (2000) The binding of myristoylated *N*-terminal nonapeptide from neuron-specific protein CAP-23/NAP-22 to calmodulin induces a 'relaxed' globular structure different from the calmodulin—non-myristoylated peptide complex. Protein Sci 86:1905–1913

Jafari MR, Deng L, Kitov PI, Ng S, Matochko WL, Tjhung KF, Zeberoff A, Elias A, Klassen JS, Derda R (2014) Discovery of light-responsive ligands through screening of a light-responsive genetically encoded library. ACS Chem Biol 9:443–450

Lane MD, Seeling B (2014) Advances in the directed evolution of proteins. Curr Opin Chem Biol 22:129–136

Li S, Roberts RW (2003) A novel strategy for in vitro selection of peptide-drug conjugates. Chem Biol 10:233–239

Lin YM, Liu YP, Cheung WY (1974) Cyclic 3′-5′-nucleotide phosphodiesterase-purification, characterization and active form of protein activator from bovine brain. J Biol Chem 249:4943–4954

Liu M, Tada S, Ito M, Abe H, Ito Y (2012) In vitro selection of a photo-responsive peptide aptamer by ribosome display. Chem Commun 48:11871–11873

Maini R, Umemoto S, Suga H (2016) Ribosomal-mediated synthesis of natural product-like peptides via cell-free translation. Curr Opin Chem Biol 34:44–52

Manandhar Y, Bahadur KCT, Wang W, Uzawa T, Aigaki T, Ito Y (2015) In vitro selection of a peptide aptamer that changes fluorescence in response to verotoxin. Biotechnol Lett 37:619–625

Nemoto N, Miyamoto-Sato E, Husimi Y, Yanagawa H (1997) In vitro virus: bonding of mRNA bearing puromycin at the 3′-terminal end to the *C*-terminal end of its encoded protein on the ribosome in vitro. FEBS Lett 414:405–408

Roberts RW, Szostak JW (1997) RNA-peptide fusions for the in vitro selection of peptides and proteins. Proc Natl Acad Sci USA 94:12297–12302

Smith GP (1985) Filamentous fusion phage: novel expression vectors that display cloned antigens on the virion surface. Science 228:1315–1317

Ueno S, Yoshida S, Mondal A, Nishina K, Koyama M, Sakata I, Miura K, Hayashi Y, Nemoto N, Nisigaki K, Sakai T (2012) In vitro selection of peptide antagonist of growth hormone secretagogue receptor using cDNA display. Proc Natl Acad Sci USA 109:11121–11126

Uzawa T, Tada S, Wang W, Ito Y (2013) Expansion of aptamer library from "Natural soup" to "Unnatural soup". Chem Commun 49:1786–1795

Wang W, Hirano Y, Uzawa T, Liu M, Taiji M, Ito Y (2014a) In vitro selection of a peptide aptamer that potentiates inhibition of cyclin-dependent kinase 2 by purvalanol. Med Chem Commun 5:1400–1403

Wang W, Uzawa T, Tochio N, Hamatsu J, Hirano Y, Tada S, Saneyoshi H, Kigawa T, Hayashi N, Ito Y, Taiji M, Aigaki T, Ito Y (2014b) A fluorogenic peptide probe developed by in vitro selection using tRNA carrying a fluorogenic amino acid. Chem Commun 50:2962–2964

Wang W, Zhu L, Hirano Y, Karamiavargani M, Tada S, Zhang G, Uzawa T, Zhang D, Hirose T, Taiji M, Ito Y (2016) Fluorogenic enhancement of in vitro selected binding peptide ligand by replacement of fluorescent group. Anal Chem 88:7991–7997

Wilke P, Helfrich N, Mark A, Papastavrou G, Faivre D, Börner HG (2014) A direct biocombinatorial strategy towards next generation, mussel-glue inspired saltwater adhesives. J Am Chem Soc 136:12667–12674